12. W. Demtröder, *Laser Spectroscopy: Basic Concepts and Instrumentation* (Springer-Verlag, New York, 1982).
13. D. P. Gerrity and J. J. Valentini, *J. Chem. Phys.* **79**, 5202 (1983).
14. G. S. Hurst, M. H. Nayfeh, J. P. Young, M. G. Payne, L. W. Grossman, in *Laser Spectroscopy III*, J. L. Hall and J. L. Carlsten, Eds. (Springer-Verlag, New York, 1977), p. 44.
15. R. Hilbig and R. Wallenstein, *Appl. Opt.* **21**, 913 (1982).
16. M. Kneba and J. Wolfrum, *Annu. Rev. Phys. Chem.* **31**, 47 (1980).
17. I. W. M. Smith, in *Physical Chemistry of Fast Reactions*, I. W. M. Smith, Ed. (Plenum, New York, 1980), vol. 2, pp. 1–82.
18. Z. Karny and R. N. Zare, *J. Chem. Phys.* **68**, 3360 (1980).
19. C.-K. Man and R. C. Estler, *ibid.* **75**, 2779 (1981).
20. B. E. Holmes and D. W. Setser, in *Physical Chemistry of Fast Reactions*, I. W. M. Smith, Ed. (Plenum, New York, 1980), vol. 2, pp. 83–214.
21. R. Altcorn, F. E. Bartoszek, J. DeHaven, G. Hancock, D. S. Perry, R. N. Zare, *Chem. Phys. Lett.* **98**, 212 (1983).
22. S. R. Leone, *Annu. Rev. Phys. Chem.* **35**, 109 (1984).
23. W. H. Breckenridge and H. Umemoto, *J. Chem. Phys.* **80**, 4168 (1984).
24. A. C. Luntz, *ibid.* **73**, 1143 (1980).
25. W. A. Guillory, K. H. Gericke, F. J. Comes, *ibid.* **78**, 5993 (1983).
26. E. E. Marinero, C. T. Rettner, R. N. Zare, *ibid.* **80**, 4142 (1984).
27. C. A. Wight, F. Magnotta, S. R. Leone, *ibid.* **81**, 3951 (1984).
28. E. E. Ferguson, F. C. Fehsenfeld, A. L. Schmeltekopf, *Adv. At. Mol. Phys.* **5**, 1 (1969).
29. L. Hüwel, D. R. Guyer, G. H. Lin, S. R. Leone, *J. Chem. Phys.* **81**, 3520 (1984).
30. C. E. Hamilton, G. H. Lin, J. Maier, V. M. Bierbaum, S. R. Leone, in preparation.
31. D. R. Guyer, L. Hüwel, S. R. Leone, *J. Chem. Phys.* **79**, 1259 (1983); C. E. Hamilton, V. M. Bierbaum, S. R. Leone, in preparation.
32. J. W. Hepburn, K. Liu, R. G. Macdonald, F. J. Northrup, J. C. Polanyi, *J. Chem. Phys.* **75**, 3353 (1981).
33. H.-J. Yuh and P. J. Dagdigian, *ibid.* **79**, 2086 (1983).
34. R. N. Zare, *Ber. Bunsenges. Phys. Chem.* **86**, 422 (1982).
35. S. Stolte, *ibid.*, p. 413.
36. T. Rettner and R. N. Zare, *J. Chem. Phys.* **77**, 2416 (1982).
37. Z. Karny, R. C. Estler, R. N. Zare, *ibid.* **69**, 5199 (1978).
38. K. Kleinermanns and J. Wolfrum, *ibid.* **80**, 1446 (1984).
39. P. R. Brooks, R. F. Curl, T. C. Maguire, *Ber. Bunsenges. Phys. Chem.* **86**, 401 (1982).
40. P. Arrowsmith, S. H. P. Bly, P. E. Charters, J. C. Polanyi, *J. Chem. Phys.* **79**, 283 (1983).
41. C. Jouvet and B. Soep, *Chem. Phys. Lett.* **96** 426 (1983).
42. I am grateful for support from the National Bureau of Standards, National Science Foundation, Air Force Office of Scientific Research, Department of Energy, and Army Research Office.

Understanding Molecular Dynamics Quantum-State by Quantum-State

Warren D. Lawrance, C. Bradley Moore, Hrvoje Petek

Summary. It is now possible to resolve completely the initial and final quantum states in chemical processes. Spectra of reactive intermediates, of highly vibrationally excited molecules, and even of molecules in the process of falling apart have been recorded. This information has led to greater understanding of the molecular structure and dynamics of small gas-phase molecules. Many of the concepts and spectroscopic techniques that have been developed will be valuable throughout chemistry.

The process of energy transfer within a molecule or group of molecules is closely related to the making and breaking of chemical bonds. Although it is not possible to photograph step-by-step motions of individual atoms and molecules, it is possible to resolve individual quantum states in the observation of molecular spectra, in the preparation of reactant molecules, and in the analysis of reaction products.

Such information, in combination with theory, reveals a great deal about the dynamics of atomic and molecular motions and about the potential energy surfaces that govern them. In an article in this issue, Leone (*1*) discusses bimolecular reactions in the gas phase. Our article deals with unimolecular processes, including the nature of excited states and reaction intermediates as revealed by their spectra, the dynamics of intramolecular vibrational energy redistribution as probed by spectroscopy, and the dynamics of photofragmentation as resolved quantum-state by quantum-state. We have selected a few examples to illustrate the power of some of the new types of experiments and of the tools now available, but much equally important and interesting work is not discussed.

Warren D. Lawrance is an Adolf C. and Mary Sprague Miller Institute postdoctoral fellow in the Chemistry Department at the University of California, Berkeley, and a guest scientist at the Materials and Molecular Research Division of the Lawrence Berkeley Laboratory, Berkeley, California 94720. C. Bradley Moore is professor and chairman of the Chemistry Department at the University of California, Berkeley, and faculty senior scientist with the Materials and Molecular Research Division of the Lawrence Berkeley Laboratory. Hrvoje Petek is a National Science Foundation predoctoral fellow in the Chemistry Department at the University of California, Berkeley.

Spectroscopy of Transient Molecules

Lasers have made it possible to observe the spectra and study the dynamics and chemical kinetics of many free radicals (*2, 3*), ions (*2, 4*), molecular excited states, and other transient species (*2*). Frequency resolution as high as 1 part in 10^8 is possible. Lasers with pulses as brief as 10^{-14} to 10^{-13} second access the shortest chemically significant time scales, for which the energy uncertainty, $\Delta E \sim \hbar/\Delta t$, is comparable to chemical bond energies (*3, 5*). Sensitivities sufficient to detect single molecules have been demonstrated for more modest limits of spectral and temporal resolution (*6*).

Methylene (CH_2), the prototype for divalent carbon intermediates, has been the focus of many experimental and theoretical studies aimed at determining the structure and the energy separation of the two low-lying electronic states, the "metastable" singlet ($^1CH_2$) and the ground triplet ($^3CH_2$) states. Spectroscopic detection of methylene eluded experimentalists for many years during which the only evidence for the theoretically postulated electronic structure of methylene was the vastly different chemistry exhibited by the two electronic spin states (*3*). In an article in this issue, Goddard (*7*) discusses the interaction between experiment and theory that produced accurate determinations of both the singlet and triplet structures, as well as the value of 9 kcal/mol for the energy separation between the singlet and triplet states (Δ_{s-t}).

The pioneering flash-kinetic spectroscopy work of Herzberg provided the first spectra and structure for triplet methylene and showed that it is the ground state (*8*). Laser magnetic resonance, a technique whereby rotational or

vibrational transitions are brought into resonance with a fixed infrared laser frequency by magnetic tuning of fine-structure transitions, has been used to detect spectra of several isotopomers of triplet methylene (*9*). The $^3CH_2$ structure and potential energy surface derived from these data indicate a bent structure with a barrier to linearity of 1950 cm^{-1} (*9*), in excellent agreement with state of the art quantum chemical calculations (*7*).

The analysis of the visible spectrum of $^1CH_2$ by Herzberg and Johns (*8*) indicates a transition from a bent lower state to a linear upper state. In a recent reinvestigation of this spectrum, ultraviolet laser photolysis of ketene was used to generate a large density of $^1CH_2$, and narrowband tunable infrared or visible lasers were used to probe the absorption spectrum (Fig. 1) (*10, 11*). This modern version of flash-kinetic spectroscopy, in which traditional photolysis and probe flash lamps have been replaced by lasers, has resulted in significantly greater sensitivity and better wavelength resolution, as well as extension to the infrared—the spectral region from which important structural information for most molecules is readily obtained. The detection of the symmetric and antisymmetric stretch spectra of an extremely reactive molecular transient such as $^1CH_2$ (*11*) demonstrates the utility of this technique for structural and time-resolved studies of short-lived species. The structure of $^1CH_2$ determined by analysis of the visible and infrared spectra improves on the original work of Herzberg and Johns and agrees well with theoretical work (*10, 11*).

The detailed analysis of singlet methylene spectra leads to two significant conclusions (*10, 11*): (i) many calculated transition frequencies are shifted from their observed positions, and (ii) there are many extra transitions not predicted by calculations. This indicates strong coupling between the singlet and triplet manifolds. The simplest spectral manifestation of these perturbations would be a doubling and shifting of optical transitions as a result of the mixing of singlet and triplet quantum states by coupling between electron spin and orbital angular momenta. These mixed states exhibit both singlet and triplet characteristics; the singlet character gives intensity to otherwise forbidden singlet-triplet optical transitions, and the triplet character is expressed by the states having a Zeeman effect arising from the interaction of an external magnetic field with unpaired electron spins of the triplet electronic state component.

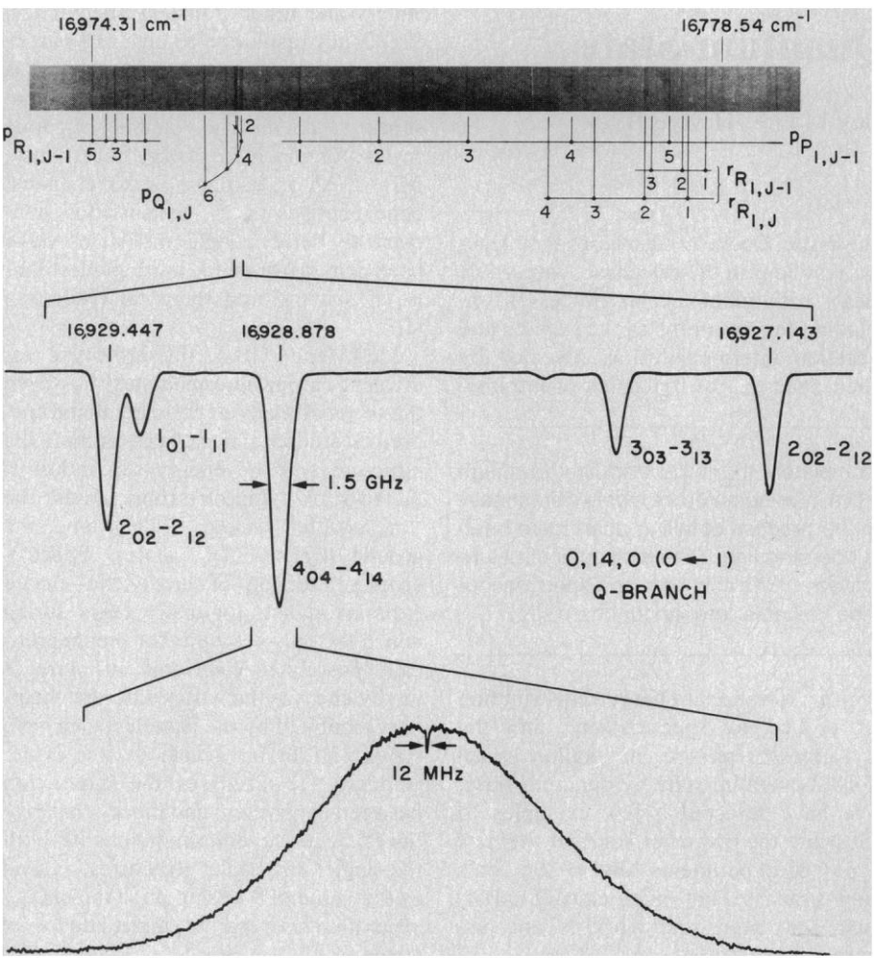

Fig. 1. Flash kinetic spectra of singlet methylene. The electronic transition is $\tilde{b}\ ^1B_1 \leftarrow \tilde{a}\ ^1A_1$. The region presented shows part of the rotational structure of the (0,14,0) ← (0,0,0) vibrational transition that accompanies this electronic excitation [(n_1,n_2,n_3) refers to the number of quanta in the vibrations ν_1, ν_2, and ν_3, respectively]. From top to bottom: the original photographic plate of Herzberg and Johns showing the P, Q, and R branches; middle, the Q-branch Doppler-limited spectrum; bottom, the sub-Doppler Lamb dip feature on the 4_{04}–4_{14} transition. The width of the Lamb dip corresponds to 5 parts in 10^7 frequency resolutions. [Courtesy of *Proceedings of the Royal Society (London)*, in G. Herzberg and J. W. C. Johns (*8*)].

These perturbations were first observed by laser magnetic resonance for four rotational transitions of excited bending vibrational states of triplet methylene (*9*). The analysis of the anomalous Zeeman effect (decrease in magnetic dipole) induced by singlet mixing provided the assignment of these perturbations and the most precise value to date for the singlet-triplet energy difference. The assignment of these perturbations has been confirmed by the visible and infrared spectroscopy of singlet methylene (*10, 11*). Many other perturbations have been detected by magnetic rotation spectroscopy, an extremely sensitive technique that relies on the rotation of the polarization of the probing light by transitions that are Zeeman-active in an external magnetic field (*12*). Some of these singlet states couple to the fundamental stretching vibrations of $^3CH_2$. Observation of the CH stretching infrared spectra of $^3CH_2$ can provide a determination of Δ_{s-t} accurate to 0.01 cm^{-1}. Such accuracy should challenge quantum chemical calculations for some time.

Very recently, sub-Doppler resolution has been achieved for flash-kinetic spectroscopy of methylene (*13*). This will permit an extensive quantitative study of singlet-triplet perturbations. Normally the resolution of molecular spectra is intrinsically limited by the frequency shift due to the thermal motion of the molecules (Doppler effect). Much higher resolution can be achieved by the use of saturation spectroscopy techniques with a narrow-frequency-width laser. The Zeeman effect splits each rotational line into magnetic fine-structure components and gives a quantitative measure of triplet admixture in these states.

These singlet-triplet perturbations have significant consequences for the dynamics of methylene. The collisional quenching of singlet to triplet methylene by inert collision partners occurs efficiently (*14*). Gelbart and Freed (*15*) describe collision-induced singlet-triplet quenching in terms of vibrational and

rotational energy transfers between mixed singlet and triplet levels, followed by vibrational relaxation in the manifold of the lower-energy electronic state. Thus the intramolecular perturbations provide the pathway for a collisional energy transfer that is forbidden by strict spin conservation rules.

Other dynamic manifestations of singlet-triplet couplings can be seen in the chemistry of methylene. The reaction

$$^3CH_2 + CH_4 \rightarrow \text{products}$$

exhibits an activation energy of 10 ± 2 kcal/mol (*16*). Since collisional interconversion between $^1CH_2$ and $^3CH_2$ is facile and the reaction of $^1CH_2$ with methane has a nearly gas kinetic rate constant (*14*), the observed activation energy is approximately equal to the value of Δ_{s-t} required to produce $^1CH_2$ from ground state $^3CH_2$ by collisional excitation.

The observation of strong coupling between the two low-lying electronic states has significantly increased our understanding of methylene structure and dynamics and has made necessary a reevaluation of previous work on methylene kinetics. The detailed understanding of this coupling and the collision-induced relaxation mediated by the perturbed states are important for understanding similar processes in larger molecules.

Intramolecular Vibrational Energy Redistribution

In any process involving chemical change there is a making or breaking of chemical bonds. Unimolecular reactions are the simplest of chemical reactions because the bond breaking occurs in the isolated molecule. When thermal collisions are used to excite a molecule above its dissociation energy, all of the vibrational motions are excited, even though only one or two bonds are usually broken. If it were possible to excite only those bonds that one wished to break, very specific and interesting new chemistry could be performed. This possibility has proved to be difficult to realize (*17*).

Vibrational spectroscopy is based on the observation that, at low energy, molecules have distinct vibrations, referred to as normal modes, in which the atomic nuclei have quite different motions that involve the stretching or bending of specific bonds. In this region the potential energy surface can be approximated by a sum of individual parabolas, one for each normal mode. Thus each normal mode is a separate vibrational oscillator. The terms that are omitted in this so-called harmonic approximation are referred to as vibrational anharmonicity and are quite small at low energy. In contrast with this ordered picture at low energy, the almost universally successful theory of thermal unimolecular reactions is based on the assumption that, at the energies of dissociation, vibrational energy is not confined to specific nuclear motions and is free to exchange among different bonds. This exchange of vibrational energy among different vibrational modes, which is referred to as intramolecular vibrational redistribution (IVR), arises when the vibrational modes are no longer isolated oscillators but are coupled together by effects such as anharmonicity. The possibilities for mode-specific chemistry are determined by where and how these two different vibrational regimes merge; to achieve mode-specific chemistry requires that the IVR rate be slower than the reaction rates. Consequently, the study of IVR is central in the study of chemical dynamics.

At low energies there is no time evolution in the vibrational motion because each of the spectral features excited is a molecular eigenstate (that is, a stationary-state solution of Schrödinger's equation). However, at higher energies the molecular eigenstates are a mixture of normal modes because of the coupling referred to above. If all of the states that share the character of a particular normal mode are excited in unison (coherent excitation), the wave functions for the states begin "in phase," so that the sum of all of the atomic displacements corresponds to that normal mode. However, because the energy of each of the states is slightly different, the wave functions each have a slightly different frequency and, with time, shift out of phase. When they are out of phase, the constructive and destructive interference that led to the initial appearance of the normal mode vanishes, and the molecule takes on a new vibrational motion. The IVR rate is the rate at which this dephasing occurs. It is dependent on how strongly the modes are coupled (how mixed the states are) and on the energy spread between the coupled states.

Much of our knowledge of what determines the onset of IVR comes from fluorescence studies at low vibrational energies (typically <6000 cm^{-1}). The fluorescence spectrum for a particular vibrational motion serves as a fingerprint for that motion. Spectral features arising from excitation of vibrations that do not contribute to the intensity of the absorption indicate that IVR is occurring. This technique has been explored in both ground and excited electronic states.

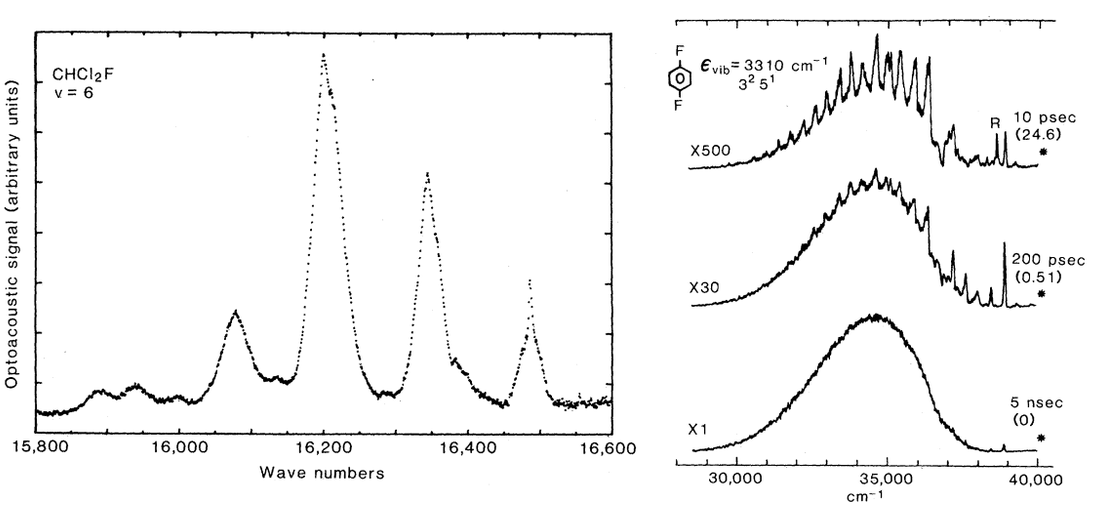

Fig. 2 (left). The $v_{CH} = 6 \leftarrow 0$ photoacoustic spectrum for CH stretching in $CHCl_2F$. One band would be observed in the absence of coupling; however, the $v_{CH} = 6$ level is strongly coupled to levels with $v_{CH} = 5$ and $v_{bend} = 2$. Fig. 3 (right). Fluorescence emission after pumping the $3_0^2 5_0^1$ absorption band of *p*-difluorobenzene (vibrational energy, 3310 cm^{-1}) with three different pressures of O_2 present. Fluorescence lifetimes and O_2 pressures (kilotorrs, in parentheses) are shown on the right. The feature marked R is Raman scattering from O_2. The laser excitation energy is marked with an asterisk. At short times emission from $3^2 5^1$ is seen; however, at long times this emission is swamped by emission from other levels that are populated by redistribution from $3^2 5^1$.

There are two experimental approaches. The first involves exciting the same, or similar, vibrations in a number of related molecules in order to see the effect of increasing the vibrational state density by increasing the molecular complexity. Smalley (*18*) and his co-workers, for example, performed experiments on a series of alkylbenzenes. They found that an increase in the length of the alkyl side chain results in an increase in emission from states with no absorption intensity. Stewart and McDonald (*19*) studied the CH stretch fundamental in various molecules and showed that there is a definite correlation between the extent of IVR and the number of near-resonant states having the correct symmetry to couple. The second approach is to probe the extent of IVR from different vibrational levels of the same molecule (*20*). In this case, a steady increase in IVR with the density of vibrational states is particularly obvious. Spectra at low vibrational energy show the structure expected; however, as the vibrational energy increases there is a growth in emission from nearby states until finally all semblance of structure from the excited level vanishes. The conclusion from the large number of different experiments is that the onset of IVR is a function of the density of states of the correct symmetry surrounding the excited level. However, the range of state densities for which IVR begins will most certainly vary among different classes of molecules and types of vibrations.

Information concerning the coupling mechanisms that are most important in the onset of IVR is beginning to emerge. In this region, mixing of individual states may be observed with high-resolution spectroscopy. Field and Kinsey and their associates (*21*) have studied the interactions among vibration-rotation levels as a function of vibrational and rotational excitation, in a series of experiments on formaldehyde and acetylene in which they used the technique of stimulated emission pumping. This technique is used to reach the high vibrational levels of the ground electronic state (S_0) in a two-step process: molecules are first excited to a specific vibration-rotation level in the first excited electronic state (S_1) and then transferred to S_0 by stimulated emission. Because a single state is prepared in S_1, only one to six rotational transitions can accompany a given vibrational transition, resulting in a simple and easily assigned spectrum of the S_0 levels. Any lines that are observed but not predicted by the selection rules for optical transitions arise from couplings among the S_0 levels. The formaldehyde data show conclusively that both anharmonic coupling, a purely vibrational effect, and Coriolis coupling, an effect arising from the interaction of rotational and vibrational motion, contribute to the vibrational state mixing. Furthermore, it is seen that Coriolis coupling effects begin to dominate the spectra as the rotational quantum numbers J and K increase. It is clear that rotational excitation can increase the coupling among the vibrational states and hence the rate of IVR.

Studies at energies approaching those of chemical relevance have focused on the behavior of the CH stretching motion, primarily because the combination of high energy and large anharmonicity possessed by these modes is the most favorable for direct excitation. Photoacoustic spectroscopy is used to detect the absorption spectra of these highly excited states. The width of each absorption feature can be interpreted as the time it takes for the excitation to transfer from the CH stretch to other vibrational motions. The broad line widths (of order 10^2 cm^{-1}) observed at high overtones (typically the vibrational energy is in the range of 10,000 to 20,000 cm^{-1}) indicate redistribution times of the order of 10^2 femtoseconds. Berry and his associates (*22*) have shown that the line widths of CH overtones in benzene first increase with increasing energy as expected on the basis of increasing state density, but then go through a maximum and begin decreasing. Thus it appears that the vibrational redistribution rates do not simply increase monotonically with energy. These results have been interpreted by Sibert *et al.* (*23*) as arising from the presence of specific pathways for the vibrational energy flow from mode to mode. They suggest that the CH stretch and CCH in-plane wag motions are intimately connected through a strong Fermi resonance (anharmonic coupling) and that excitation of the stretch is quickly transferred to a combination of stretch and wag motions. This transfer requires a proximity of the energy of the vibrations. As the overtone excitation increases, the anharmonicity of the CH

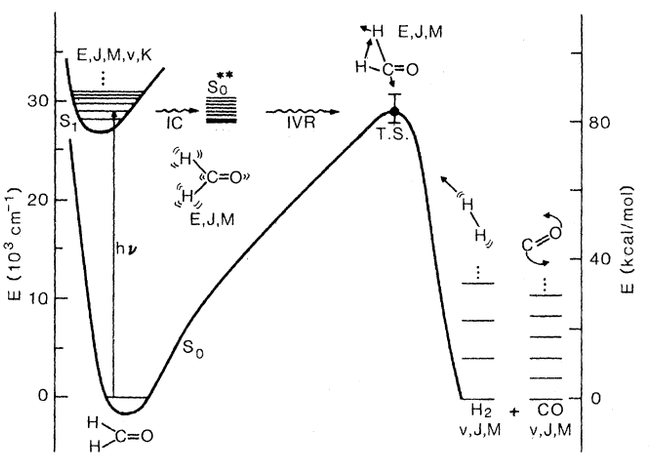

Fig. 4 (left). Energy states along the reaction coordinate for photofragmentation of H_2CO to H_2 and CO. Abbreviations: *IC*, internal conversion; *T.S.*, transition state. *E* refers to the energy; *v* to vibrational quantum numbers; and *J*, *M*, and *K* to rotational quantum numbers. Fig. 5 (right). A Boltzmann plot of the rotational distribution of the CO photofragment from formaldehyde photolysis near 29,500 cm^{-1}. Curves through the data are drawn by hand. H_2 pushes off from the electron distribution outside the carbon nucleus, imparting a large angular momentum to CO. [Courtesy of *Journal of Chemical Physics* (*33*)].

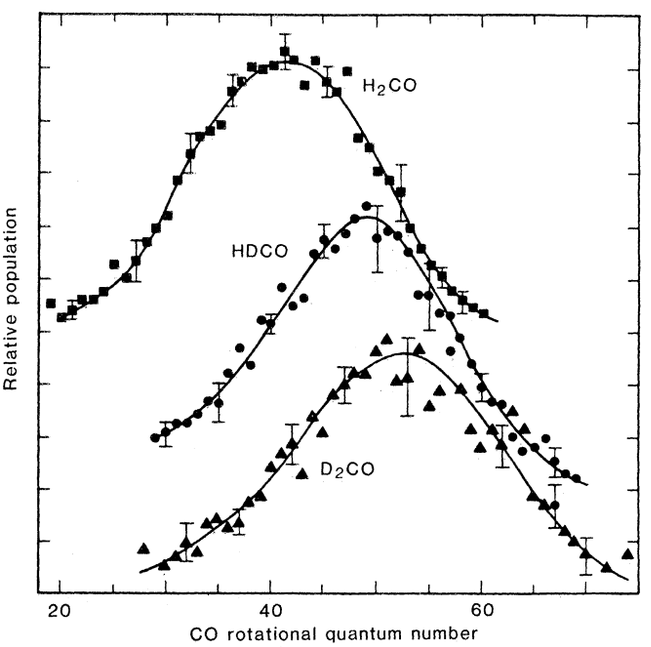

overtone alters the energy separation, first causing an increase in the interaction as the levels approach in energy, and then a decrease as they pass each other.

This kind of mechanical resonance in IVR should be quite general in CH overtone spectra, and for this reason several groups of investigators are gathering precise data on the closely related CH stretch–CH bend interaction (*24, 25*). For the trihalomethanes (*24*), the presence of a single CH chromophore and a small number of vibrational modes considerably simplifies the spectra. For example, the strong interaction between the CH stretch and CH bend is clearly demonstrated by the presence of four strong absorption features rather than one for the fifth CH stretch overtone of $CHCl_2F$ (Fig. 2). An analysis of the spectra in terms of a cubic anharmonic coupling between the stretch and bend modes reproduces the observed band positions and intensities. It is clear from this analysis that the interaction between the CH stretch and CH bend is the dominant influence. Furthermore, the coupling constant obtained from the analysis can be broken down into two contributions, the intrinsic anharmonicity of the potential surface for the CH bond, the calculation of which requires extensive ab initio computations, and the more easily calculable kinetic anharmonicity induced by the pendulum-like motion of the CH bend. The kinetic anharmonicity is the largest contribution to the coupling (*24*), in agreement with the assumption of Sibert *et al.* (*23*) in their calculations on benzene overtone lineshapes.

It is interesting to compare the information that can be extracted from the overtone spectra of the halomethanes and of benzene. The benzene line widths give the IVR rate for CH stretch to CCH wag, since this effect dominates the line widths; however, information concerning the redistribution to other motions is hidden by this effect. For the halomethanes, the CH stretch–CH bend interaction is separate from other coupling pathways; it appears as resolved structure in the spectra. The IVR rate for CH stretch to CH bend can be calculated from these data. The line widths of the isolated features give the magnitude of the strongest coupling of the CH modes to other vibrational motions. It is clear that the motions of the halogens are much less strongly coupled, and the IVR lifetime is correspondingly much longer than for the CH stretch to CH bend energy transfer.

These overtone spectra, and their interpretation in terms of specific pathways for redistribution, highlight the existence of wide variation in the coupling strengths of different types of nuclear motion. This finding is encouraging for those interested in trying to implement reaction along a particular coordinate.

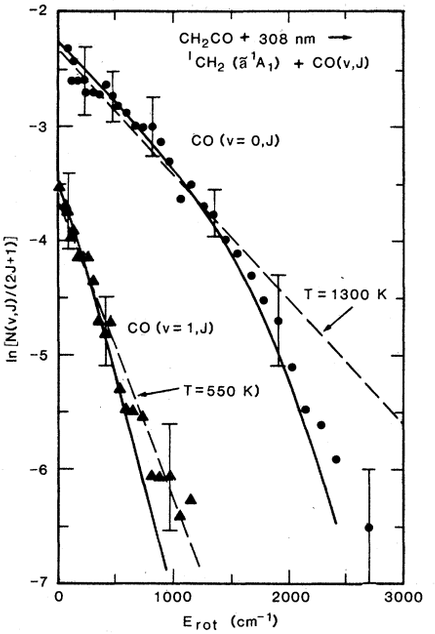

Fig. 6. Rotational distribution of CO fragments from ketene photolysis at 308 nm. There is no repulsion between the CH_2 and CO fragments. The solid curves are calculated without any adjustable parameters, on the assumption that all energetically accessible product states have equal probability.

All of the IVR experiments discussed so far are time-independent. However, the most spectacular view of IVR comes from direct time domain experiments in which the evolution of vibrational motion from the initially prepared state to the surrounding states is monitored. Although experiments on a picosecond time scale are difficult to perform and lie at the forefront of technology, such measurements are now being performed (*26, 27*). The largest data set for IVR rates, however, resulted from an ingenious method devised by Parmenter (*20, 28*). This method, called "chemical timing," has been used to obtain spectra on a picosecond time scale without recourse to picosecond technology. A high pressure of an electronic state quencher is used to shorten the lifetime of the emitting state to as little as 10 picoseconds, so that only molecules that fluoresce promptly (before undergoing a collision with the quencher) are observed. The spectrum at very short times (that is, at high pressure of the quencher) is just that which is characteristic of the coordinates excited. At longer times (low quencher pressure) there is a relative decrease in this emission and a corresponding increase in a broad emission which results following the transfer of energy from the vibrational mode initially prepared. By varying the pressure of the quencher, one can select molecules with a particular lifetime to obtain a view of the evolution of the vibrational motion. An example of the behavior observed is shown in Fig. 3. Lifetimes for IVR (inverse of the IVR rates) extracted for the low vibrational levels studied (<3500 cm^{-1}) range from nanoseconds to tens of picoseconds. The exact mechanism by which the "chemical timing" process works is unknown, and the absolute accuracy of the extracted rates remains in question. However, it is clear from recent direct picosecond experiments by Hochstrasser and his co-workers (*26*) and by Felker and Zewail (*27*) that the rates are of the right order of magnitude.

Photofragmentation Dynamics

When a diatomic molecule is photoexcited to a repulsive electronic state (potential curve), it dissociates in one-half of a molecular vibration to atomic fragments in states corresponding to that curve and with a translational energy specified by energy conservation. Excitation to a bound excited electronic state results in fluorescence back to vibrational levels of the ground electronic state or in predissociation by crossing (nonradiative transition) to a repulsive electronic curve, or both. The potential surfaces of polyatomic molecules are much more complex; each added atom increases the dimension by three. This increase in complexity opens many new pathways for energy flow from the initial excitation to reaction products. Crossing from a completely bound potential surface to one with an energetically accessible exit valley may occur. A molecule with sufficient energy to dissociate on a given surface may execute many vibrations before passing through an exit valley of the surface to fragments. Molecular fragments may be vibrationally and rotationally excited as well as electronically excited. Thus there are many fragment-state quantum numbers to be determined. The fragment vibration, translation, and both magnitude and direction of angular momentum may be expected to depend on (i) the initial angular momentum and vibrational excitation, (ii) the nature of any transitions between potential surfaces, (iii) coupling among degrees of freedom of the excited molecule, (iv) the geometry of the "tran-

sition state," and (v) the shape of the potential surface in the exit valley. Recent results on H_2CO, CH_2CO, and NCNO illustrate how dynamic information may be derived from high-resolution photofragment spectroscopy (*29*).

The formaldehyde molecule (Fig. 4) provides an opportunity for complete spectroscopic resolution and theoretical study of polyatomic molecule dissociation (*30*). The near ultraviolet $\pi^* \leftarrow n$ excitation of the carbonyl of formaldehyde gives a bound singlet state (S_1). The spectrum is completely resolvable, and therefore a pulsed, narrowband laser produces S_1 with all vibrational and rotational quantum numbers defined. This excited state internally converts to a highly vibrationally excited ground singlet state (S_0**) with conservation of total energy and angular momentum, E and J. This transfer from electronic to vibrational energy corresponds to curve-crossing in diatomics. S_0** then vibrates until nearly all of the energy appears in the dissociation coordinate to bring the molecule to the transition state. The geometry and energy of this transition state have been established to good accuracy by extensive ab initio calculations (*31*). We describe here experiments that used a total energy just a few kilocalories per mole above this barrier. Some 80 kcal/mol are then released as the H_2 and CO fragments push off from each other.

Table 1. Average energy in each degree of freedom for photofragmentation of H_2CO.

Fragment	Average energy (%)		
	Translation	Rotation	Vibration
CO	4	13	1
H_2	61	5	16

The vibration-rotation-translation states of the fragments are probed spectroscopically. Molecular-beam time-of-flight spectroscopy shows that most of the energy (65 percent on average) goes into translation (*32*). Laser-excited vacuum ultraviolet fluorescence detection of the rotation-vibration states of the nascent CO product shows that CO is highly rotationally excited (Fig. 5) (*33*). The most probable value of the rotational quantum number J for CO is 42 (49 and 53 for HDCO and D_2CO, respectively) independent of the initial rotational excitation of the H_2CO for the two levels studied (for which J = 3 and 16). In comparison, the most probable value of J for CO at room temperature is 7. Those few percent of CO molecules formed in vibrational level v = 1 exhibit the same rotational distribution as those in v = 0. H_2 is observed by coherent antistokes Raman spectroscopy (*34*). The distribution of vibrational energy is found to be v = 0 (23 percent), v = 1 (43 percent), v = 2 (25 percent), v = 3 (9 percent), and v = 4 ($\leq$1 percent). The rotational distributions of H_2 peak at J = 5 and correspond roughly to temperatures that vary from 1800 K for v = 3 to 3000 K for v = 0. Nuclear spin is found to be conserved in the dissociation process (*34*); only odd J (that is, ortho) H_2 is produced from ortho-formaldehyde. The overall energy distribution is shown in Table 1.

The distribution of energy is dynamically controlled by the shape of the steep downhill exit valley of the potential surface; very different amounts of energy are deposited in each degree of freedom. The quantum-state distributions for H_2 vibration and CO rotation are far from thermal or statistical. The angular momentum of the CO is much greater than the initial total angular momentum. Conservation of angular momentum thus requires that J of CO be balanced by the orbital angular momentum (L) of relative motion of H_2 and CO ($J_{CO} \approx L = \mu vb$, where μ is the reduced mass of H_2 with CO, v is the relative velocity, and b the impact parameter). The mean impact parameter corresponding to J_{CO} = 42 is 0.8 Å or about 0.2 Å on the outside of the C nucleus (*33*). H_2 appears to push off from the electron cloud outside the carbon atom. The arrows on the transition state structure indicated are the reaction coordinate vectors from ab initio theory (*31*).

The fragmentation of ketene to singlet methylene and CO (*35*)

$$CH_2CO\ (S_1^*) \rightarrow CH_2CO\ (S_0^{**}) \rightarrow {}^1CH_2 + CO$$

occurs after ultraviolet excitation and internal conversion to the ground-state potential surface. The exit valley has no barrier. With excitation of 308 nm (93 kcal/mol) all of the energy except 6.7 kcal/mol is required for breaking the C=C bond (*36*). The molecule vibrates until enough energy is concentrated in

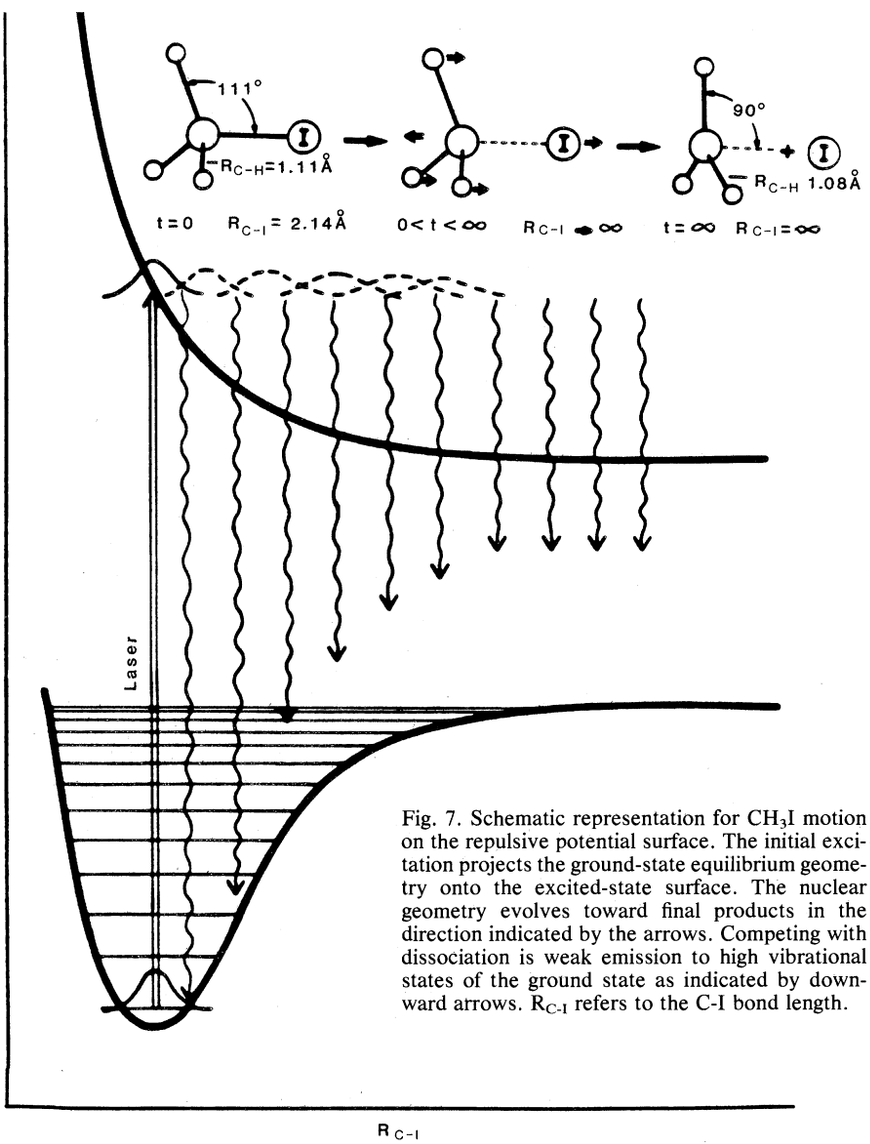

Fig. 7. Schematic representation for CH_3I motion on the repulsive potential surface. The initial excitation projects the ground-state equilibrium geometry onto the excited-state surface. The nuclear geometry evolves toward final products in the direction indicated by the arrows. Competing with dissociation is weak emission to high vibrational states of the ground state as indicated by downward arrows. R_{C-I} refers to the C-I bond length.

the dissociation coordinate so that fragments move apart. The translational energy distribution of both fragments peaks near zero (*36*). The rotational distribution of CO is roughly thermal (*35*): 1300 K for CO (v = 0) and 550 K for CO (v = 1) (Fig. 6). The rotational distributions are exactly statistical as calculated from the assumption that all energetically accessible product states have equal a priori probability. There is just enough energy for CO (v = 1) to be produced. Statistically only 1.3 percent is expected, but 29 percent population of v = 1 is observed. It appears that the soft degrees of freedom, rotation, and bends are strongly coupled and transfer energy rapidly on the time scale of the dissociation and hence are statistically controlled in the product. The CO bond stays intact through the dissociation; its behavior is different.

A study of vibration-rotation excitation of CN from

$$NCNO + h\nu \rightarrow CN + NO$$

has been carried out by Wittig and his co-workers (*37*) for photon energies from the dissociation threshold to 5000 cm^{-1} above threshold. Phase space theory, a statistical theory that is based on the assumption that energy is distributed with equal probability to all of the energetically accessible product states, is successful at matching the data for excitation energies up to 2000 cm^{-1} above the dissociation threshold. However, as soon as it is energetically possible to produce vibrational excitation of the NO and CN fragments, the phase space theory fails to reproduce the experimental CN vibration-rotation distributions. The vibrational excitation of CN is matched by a statistical calculation that distributes the excess energy among the six vibrations of a very loose NCNO transition state. The experiments give about 50 percent more molecules in v = 1 than is predicted by phase space theory, which includes all nine rotation-vibration degrees of freedom. The analogous calculation for ketone reproduces the dramatic enhancement of CO (v = 1) product (9 percent observed) above the phase space theory value (1.3 percent).

As the relations among potential surface shape, intramolecular dynamics, and photofragment energy distributions become more completely understood, it will become possible to deduce reaction mechanisms from product energy distributions. For example, it should be immediately clear from the v, J states of product CO whether a CO is eliminated in a concerted fashion from a cyclic ketone or in a stepwise process in which the CO equilibrates with the hydrocarbon fragment of a diradical before fragmenting.

So far, we have discussed experiments in which the photodissociation dynamics are studied by the observation of final product vibrational, rotational, and translational excitation. The final product energy distribution is used to infer the nuclear motion on the dissociative potential surface. Imre *et al.* (*38*) observed molecules spectroscopically during the half-vibrational period that it takes a molecule to dissociate. They excite a molecule to an unbound electronic state. The multidimensional potential energy surface for such an electronic state will have bound motion for all vibrations except the reaction coordinates. Although the molecule is dissociating in half of a vibrational period (10^{-14} second) there is a very small but observable probability of emission. Since electronic motion is much faster than nuclear motion, the light emission has the greatest probability for identical nuclear configuration of the ground and excited states. Thus emission is observed to vibrational levels of the ground electronic state that distort the molecule along the reaction coordinate. Therefore the emission spectrum shows the excitation of those ground-state vibrational modes that reflect the change in nuclear geometry as the excited state evolves into products. The intensity of the fundamental and overtone transitions has been shown by Heller (*39*) to depend on the exact shape of the potential.

The utility and elegance of this technique have been demonstrated with spectra from CH_3I and O_3 molecules excited to a dissociative continuum (*38*). The spectrum of CH_3I shows a long progression in the CI stretch (29 quanta) and in the CH_3 umbrella bending mode, reflecting the breaking of the CI bond and transformation of CH_3 from pyramidal to a planar fragment (Fig. 7). Along with the information on the excited-state potential, this technique provides spectra of very highly vibrationally excited levels of the ground electronic state that should be of great value in studying IVR.

The coming years will surely provide completely resolved dynamic studies of a significant number of small molecules. The extension of laser and synchrotron radiation technology in the vacuum ultraviolet will open Rydberg states for study. Many of the principles to be learned from these detailed studies of small gas-phase molecules will be applicable to larger molecules, to gas-surface interactions, and to condensed-phase systems.

References and Notes

1. S. R. Leone, *Science* **227**, 889 (1985).
2. T. A. Miller, *ibid.* **223**, 545 (1984).
3. K. B. Eisenthal, R. A. Moss, N. J. Turro, *ibid.* **225**, 1439 (1984).
4. C. S. Gudeman and R. J. Saykally, *Annu. Rev. Phys. Chem.* **35**, 387 (1984).
5. C. V. Shank, R. L. Fork, R. Yen, R. H. Stolen, W. J. Tomlinson, *Appl. Phys. Lett.* **40**, 761 (1982); A. M. Weiner, J. G. Fujimoto, E. P. Ippen, in *Ultrafast Phenomena IV*, D. H. Auston and K. B. Eisenthal, Eds. (Springer-Verlag, New York, 1984), p. 11.
6. R. N. Zare, *Science* **226**, 298 (1984).
7. W. A. Goddard III, *ibid.* **227**, 916 (1985).
8. G. Herzberg and J. W. C. Johns, *Proc. R. Soc. London Ser. A* **295**, 106 (1966); G. Herzberg, *ibid.* **262**, 291 (1961).
9. A. R. W. McKellar, P. R. Bunker, T. J. Sears, K. M. Evenson, R. J. Saykally, S. R. Langhoff, *J. Chem. Phys.* **79**, 5251 (1983).
10. H. Petek, D. J. Nesbitt, D. C. Darwin, C. B. Moore, in preparation.
11. H. Petek, D. J. Nesbitt, P. R. Ogilby, C. B. Moore, *J. Phys. Chem.* **83**, 5367 (1983).
12. H. Petek, D. J. Nesbitt, C. B. Moore, in preparation.
13. H. Petek, Y. Matsumoto, D. C. Darwin, D. J. Nesbitt, C. B. Moore, in preparation.
14. A. O. Langford, H. Petek, C. B. Moore, *J. Chem. Phys.* **78**, 6650 (1983).
15. W. M. Gelbart and K. F. Freed, *Chem. Phys. Lett.* **18**, 470 (1973).
16. S. Dobe, T. Bohland, F. Temps, H. Gg. Wagner, in preparation.
17. F. F. Crim, *Annu. Rev. Phys. Chem.* **35**, 657 (1984).
18. R. E. Smalley, *J. Phys. Chem.* **86**, 3504 (1982).
19. G. M. Stewart and J. D. McDonald, *J. Chem. Phys.* **78**, 3907 (1983).
20. C. S. Parmenter, *J. Phys. Chem.* **86**, 1735 (1982).
21. H. L. Dai, C. L. Corpa, J. L. Kinsey, R. W. Field, in preparation; D. E. Reisner, P. H. Vaccaro, C. Kittrell, R. W. Field, J. L. Kinsey, H. L. Dai, *ibid.* **77**, 573 (1982); E. Abramson, R. W. Field, D. Imre, K. K. Innes, J. L. Kinsey, *ibid.* **80**, 2298 (1984).
22. K. V. Reddy, D. F. Heller, M. J. Berry, *ibid.* **76**, 2814 (1962).
23. E. L. Sibert, W. P. Reinhardt, J. T. Hynes, *ibid.* **81**, 1115 (1984); *Chem. Phys. Lett.* **92**, 455 (1982).
24. W. H. Green, J. S. Wong, W. D. Lawrance, C. B. Moore, in preparation; J. S. Wong and C. B. Moore, in *Lasers and Applications*, W. O. N. Guimares, C.-T. Lin, A. Mooradian, Eds. (Proceedings of the Sergio Memorial Symposium, Rio de Janeiro, Brazil, 1980) (Springer-Verlag, New York, 1981), p. 157.
25. S. Peyerimhoff, M. Lewerenz, M. Quack, *Chem. Phys. Lett.* **109**, 563 (1984); H. R. Dubel and M. Quack, *J. Chem. Phys.* **81**, 3779 (1984).
26. R. Moore, F. E. Doany, E. J. Heilweil, R. M. Hochstrasser, *J. Phys. Chem.* **84**, 876 (1984).
27. P. M. Felker and A. H. Zewail, *Chem. Phys. Lett.* **108**, 303 (1984).
28. K. W. Holtzclaw and C. S. Parmenter, *J. Phys. Chem.* **88**, 3182 (1984); R. A. Coveleskie, D. A. Dolson, C. S. Parmenter, *ibid.*, in press.
29. For more comprehensive discussion and references, see S. R. Leone [*Adv. Chem. Phys.* **50**, 255 (1982)] and J. P. Simons [*J. Phys. Chem.* **88**, 1287 (1984)].
30. C. B. Moore and J. C. Weisshaar, *Annu. Rev. Phys. Chem.* **34**, 525 (1983).
31. J. D. Goddard, Y. Yamaguchi, H. F. Schaefer III, *J. Chem. Phys.* **75**, 3459 (1981).
32. P. Ho, D. J. Bamford, R. J. Buss, Y. T. Lee, C. B. Moore, *ibid.* **76**, 3630 (1982).
33. D. J. Bamford, S. V. Filseth, M. F. Foltz, J. W. Hepburn, C. B. Moore, *ibid.*, in press.
34. D. Debarre, M. Lefebvre, M. Pealat, J.-P. Taran, D. J. Bamford, C. B. Moore, in preparation; M. Pealat, D. Debarre, J.-M. Marie, J.-P. Taran, A. Tramer, C. B. Moore, *Chem. Phys. Lett.* **98**, 299 (1983); B. Schramm, D. J. Bamford, C. B. Moore, *ibid.*, p. 305.
35. D. J. Nesbitt, H. Petek, M. F. Foltz, S. V. Filseth, D. J. Bamford, C. B. Moore, in preparation.
36. C. C. Hayden, D. M. Neumark, K. Shobatake, R. K. Sparks, Y. T. Lee, *J. Chem. Phys.* **76**, 3607 (1982).
37. I. Nadler, M. Noble, H. Reisler, C. Wittig, *ibid.*, in press.
38. D. Imre, J. L. Kinsey, A. Sinha, J. Krenos, *J. Phys. Chem.* **88**, 3956 (1984).
39. E. J. Heller, *Acc. Chem. Res.* **14**, 368 (1981).

40. We thank C. S. Parmenter for Fig. 3 and J. L. Kinsey for Fig. 7.